The Photohydration of *N*-Alkylpyridinium Salts: Theory and Experiment

Rollin A. King,[a] Hans P. Lüthi,*[a, c] Henry F. Schaefer, III,[b] Fabrice Glarner,[c] and Ulrich Burger[c]

Abstract: Bicyclic aziridines formed by the irradiation of pyridinium salts in basic solution have recently been recognized to have great synthetic potential. We have undertaken a joint computational and experimental investigation of the mechanism of this photoreaction. We have computationally determined the structures and relative energies of the relevant stationary points on the lowest potential energy surface (PES) of the pyridinium and methylpyridinium ions. Two important intermediates are shown to be bound minima on the ground-state PES: azoniabenzvalene and a 6-aza[3.1.0]bicyclic ion with an *exo*-oriented substituent (analogous to prefulvene). We advance a mechanism which involves initial formation of this *exo*-bicyclic ion, followed by nitrogen migration around the ring via the azoniabenzvalene intermediate. Thus, the barrier separating the two intermediates is the factor that determines the degree of scrambling observed in the photoproducts when the carbon atoms are labeled with deuterium or substituted with additional methyl groups. For *N*-methylpyridinium, the *exo*-methyl bicyclic ion was computed to be ≈ 1 kcal mol^{-1} lower in energy than *N*-methyl-azoniabenzvalene. The transition state was computed to lie several kcal mol^{-1} above the *exo*-methyl bicyclic ion ($+8.4$ kcal mol^{-1}, 6-31G* RHF; $+3.7$ kcal mol^{-1}, 6-31G* B3LYP), but still well below the energy available from the 254 nm excitation of the *N*-methylpyridinium ion. The computed relative energies correspond splendidly with several experimental findings which include the preference for *exo* products, the results of deuterium labeling, and the impact of additional substituent methyl groups on the product distribution.

Keywords: ab initio calculations · aziridines · density functional calculations · pericyclic reactions · photochemistry

Introduction

In 1972, Kaplan, Pavlik, and Wilzbach[1] showed that the irradiation of *N*-methylpyridinium chloride (**1a**) in H_2O in the presence of base gave the bicyclic aziridine (±)-**2a** (Scheme 1). Their communication went relatively unnoticed for nearly a quarter of a century until it was recognized that this transformation of the pyridinium ring provides a new and powerful approach to aminocyclopentanes with well-defined substitution patterns.[2, 7] Highly functionalized aminocyclopentanes are of considerable interest as precursors of glycosidase inhibitors[8] and of carbocyclic analogues of nucleosides.[9] In fact, the photochemical step fixes the relative configuration of the three new stereogenic carbon atoms, and the resulting 6-azabicyclo[3.1.0]hex-3-en-2-ol skeleton pos-

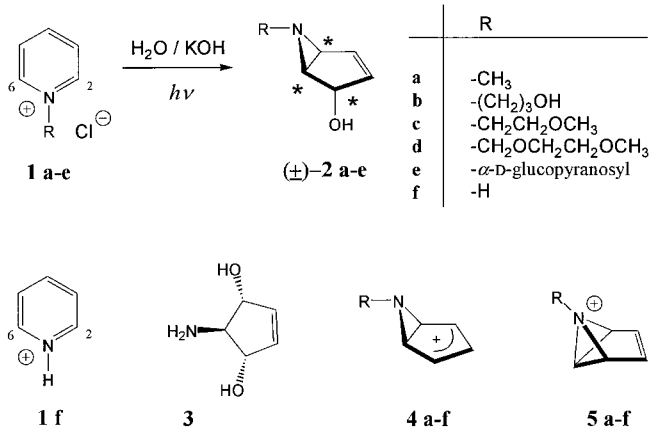

Scheme 1. Photohydration reaction of various pyridinium compounds with intermediates and products, as investigated by various groups.

[a] Priv. Doz. Dr. H. P. Lüthi, Dr. R. A. King
Laboratorium für Physikalische Chemie
Universitätsstrasse 16, ETH Zentrum
8092 Zürich (Switzerland)
Fax: (+41) 1-632-1615
E-mail: luethi@igc.phys.chem.ethz.ch

[b] Prof. H. F. Schaefer, III
Center for Computational Quantum Chemistry
University of Georgia
Athens, Georgia 30602 (USA)

[c] Priv. Doz. Dr. H. P. Lüthi, Dr. F. Glarner, Prof. U. Burger
Department of Chemistry, University of Geneva
1211 Geneva 4 (Switzerland)

Supporting information for this article is available on the WWW under http://www.wiley-vch.de/home/chemistry/ or from the author.

0947-6539/01/0708-1734 $ 17.50+.50/0

sesses intrinsic features that make it a versatile intermediate for synthesis.

Recent work has unveiled that, in place of the methyl group, N ligands bearing hydroxyalkyl, ether, or *N,O*-acetal functions (e.g., **1b–e**) are perfectly compatible with the photohydration reaction of the pyridinium ion. In the presence of a base, they all give the corresponding bridged aziridines (**2b–e**) in preparative yields ranging from 45 to 85%. Both the N ligand and the OH group adopt the "*exo*" orientation with respect to the bicyclic skeleton of these products. We note that an "*endo*" solvation has been claimed for the corresponding photoaddition of alcohols to 3-alkoxypyridinium tetrafluoroborates.[10] No bridged aziridines are formed, however, if the N substituent of the pyridinium ion contains functional groups with a low ionization potential. Under these circumstances, an entirely different reaction course prevails, which is characterized by single-electron transfer to the photoexcited pyridinium ion.[11] This course applies to carboxylate, amine, or electron-rich alkene functions.

The bridged aziridines **2a–e** have been exploited in several stereocontrolled transformations. Expansion of **2b** by transition-metal-mediated carbonylation was used in the synthesis of bridged β-lactams.[2] Opening of the three-membered ring of compounds **2** by oxygen and sulfur nucleophiles is a key reaction on the way toward aminocyclopentitols.[3, 4] Recently, the diastereomers (**2e**) resulting from the photohydration of α-D-glucopyranosylpyridinium chloride (**1e**) were resolved after peracetylation into enantiopure bridged aziridines.[7] Mariano et al.[5] have exploited the photohydration of the parent pyridinium ion (**1f**, R = H) in strong acid. Under their conditions, the in situ protonation and opening of the transient aziridine occurred to give the *meso*-cyclopentendiol amine (**3**). This compound served as starting material for a semienzymatic synthesis of mannostatin[5] and of the analogous glycosidase inhibitors.[6]

At first glance, compounds **2a–e** are formed by solvation of the corresponding 6-azabicyclo[3.1.0]hex-3-en-2-yl cation (**4a–e**) which results simply from 2,6-bridging of the excited pyridinium ion. However, as was pointed out already in the seminal publication of Wilzbach et al.,[1] the results obtained in the photohydration of 3,4,5-trideuterio-1-methylpyridinium chloride are not compatible with this simple picture. The authors invoked the intermediacy of *N*-methyl-1-azoniabenzvalene (**5a**) to account for skeletal rearrangement that precedes formation of **2a**. We comment further on these labeling experiments later in this paper. Products obtained from the photohydration of 1,2-, 1,3-, and 1,4-dimethylpyridinium chloride provided further support for the intermediacy of 1-azoniabenzvalene ions; this indicates that the methyl groups can exert a strong directive influence on their formation and fate. Nevertheless, the precise nature of the primary photoisomer of the pyridinium ion and its relationship to other reactive intermediates remained unclear.

While the photochemistry of free pyridine has been investigated both experimentally and theoretically in great detail,[12, 16] there is little theoretical work of relevance on pyridinium salts. Anthony et al.[17] have studied the attack of the OH radical on the pyridinium ion and found that the product of the attack on the *meta* position is the most stable. Del Bene and Jaffé[18] have computed the excitation spectrum of the parent pyridinium ion **1f** by means of semiempirical methods. They obtained 4.6 eV and 5.4 eV for the two lowest $\pi \rightarrow \pi^*$ excitation energies to the $^1B_2$ and $^1A_1$ symmetry states, respectively. Sobolewski and Domcke,[19] used minimal basis-set Hartree–Fock calculations to show that the bicyclic structures analogous to **4** for benzene, pyridine, and pyrazine are adiabatically correlated to valence $\pi \rightarrow \pi^*$ excited states. Thus, if any of these molecules, upon $\pi \rightarrow \pi^*$ excitation, rearranges toward a structure analogous to **4**, it will enter a region of degeneracy in which ground- and excited-state surfaces cross. Efficient, nonradiative decay of the electronic excitation takes place, and the molecule can be trapped in its electronic ground state, but in a different well on the potential energy surface (PES). Palmer et al.[20] reported higher quality computations of this process for benzene in 1993, as part of a comprehensive examination of its S_1 and S_2 photochemistry. Their work is discussed in relation to our findings in the Results and Discussion Section. In this paper, we present a joint computational and experimental analysis of the events which originate in the $\pi \rightarrow \pi^*$ excitation of the pyridinium cation. We will examine the parent pyridinium and *N*-methylpyridinium ions and then investigate the effect of *N*-methyl and selected *C*-methyl substitution.

Results and Discussion

Geometrical structures: We have computationally studied minima and transition states of both the pyridinium (**1f**) and the methylpyridinium ion (**1a**). The results are largely the same, so we explicitly discuss here only the structures for **1a**. Complete optimized geometries for the equilibrium, intermediate, and transition-state structures for both the pyridinium and methylpyridinium ions are available in the Supporting Information. The electronic structure of these minima is discussed below.

The optimized structure of the methylpyridinium ion **1a**, is shown in Figure 1. The bonds of the ring become longer as one

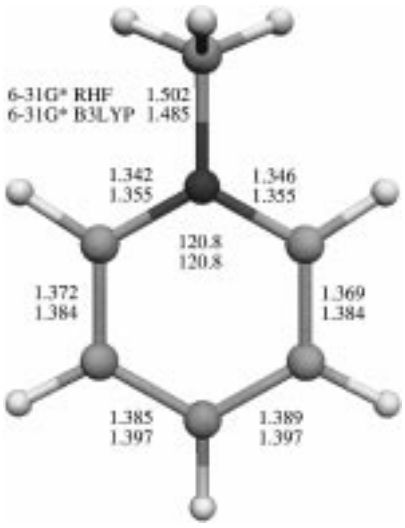

Figure 1. Geometrical structure (bond lengths in Å and bond angles in °) of the C_s symmetrical methylpyridinium minimum **1a**. The RHF structure has a rotated methyl group and a different plane of symmetry than the B3LYP structure.

progresses around the ring away from the N atom; this indicates a shift in the electron density toward the N atom. However, the N ring angle of 120.8° is hardly different from that of benzene. The RHF and B3LYP methods differ in their methyl-group orientation, so that RHF has a symmetry plane including the ring, while the symmetry plane from B3LYP is perpendicular to the ring. This difference is not significant, however, as the methyl group has virtually free rotation anyway.

The *exo*-methyl and *endo*-methyl bicyclic ions **4a** are minima on the PES and their structures are shown in Figure 2 and Figure 3, respectively. The allylic C–C bond lengths are between those of typical single and double bonds. The RHF

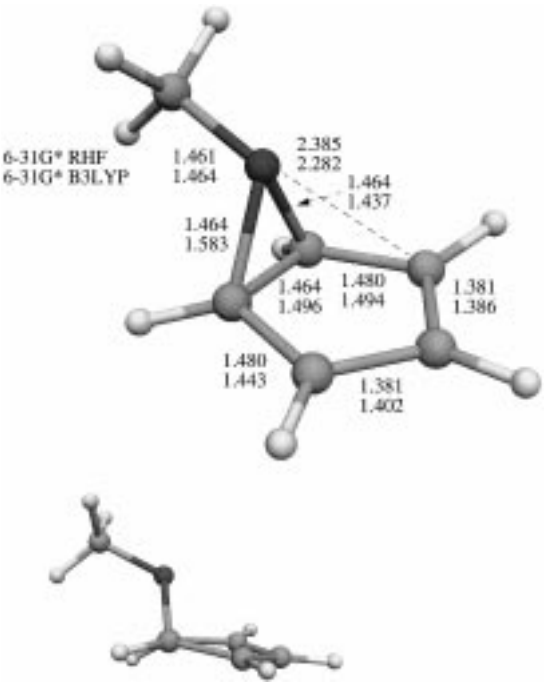

Figure 2. Geometrical structure (bond lengths in Å) of the C_s (RHF) or C_1 (B3LYP) symmetrical *exo*-methyl bicyclic ion **4a**.

method predicts C_s symmetry for both the *endo* and *exo* forms, while B3LYP predicts a slight distortion into C_1 symmetry toward an azoniabenzvalene structure. The short distance between the N and the nearest allylic C in the *exo* orientation suggests the presence of a low-energy barrier to the addition of this bond and formation of methyl-azoniabenzvalene **5a**. The C_1 point-group symmetry shown in Figure 2 is in agreement with the multiconfiguration self-consistent field (MC-SCF) minimum of the benzene analogue, "prefulvene", computed by Palmer et al.[20] It is tempting to explain this distortion by claiming that electron correlation is pointing the N lone pair toward one of the nearest allylic C atoms, since the distance for the *exo*-bicyclic ion between the N and an allylic C is only 2.3 Å. However, B3LYP also predicts a C_1 structure for the *endo*-methyl form, in which there is no lone pair above the C ring.

Figure 4 displays the computed structure for *N*-methylazoniabenzvalene (**5a**). The C–C bond opposite the N has a typical length of a double bond. The N atom has one strong

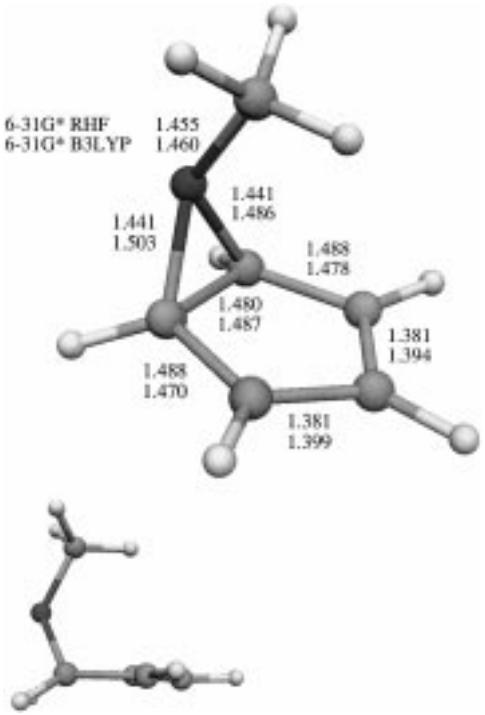

Figure 3. Geometrical structure (bond lengths in Å) of the C_s (RHF) or C_1 (B3LYP) symmetrical *endo*-methyl bicyclic ion **4a**.

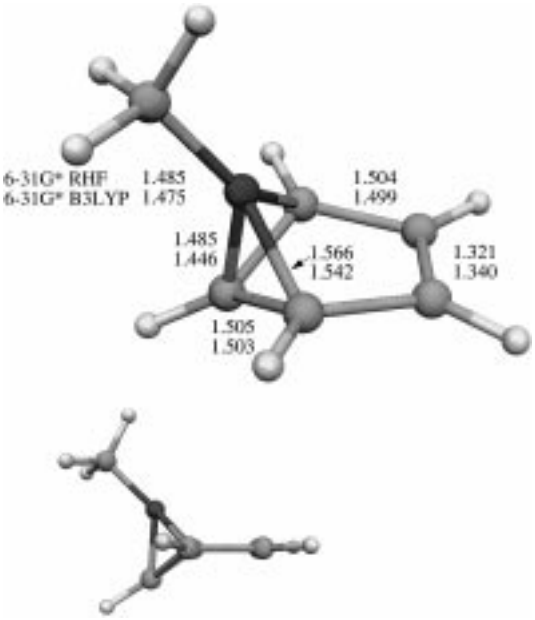

Figure 4. Geometrical structure (bond lengths in Å) of the C_s symmetrical methylazoniabenzvalene minimum **5a**.

bond to the C ring and two weaker ones. Both RHF and B3LYP predict a C_s symmetry minimum, which supports the idea that the methylazoniabenzvalene, if it reopens to a bicyclic structure, will do so in a statistical manner. Palmer et al.[20] previously computed a slightly distorted C_1 symmetry structure for benzvalene; however, they presumed (apparently correctly) that the distortion was caused by an artifact of their MC-SCF active space.

A computational search was also made for hypervalent intermediates in which the N is bonded to more than three C

0947-6539/01/0708-1736 $ 17.50+.50/0 *Chem. Eur. J.* **2001**, *7*, No. 8

ring atoms. However, all attempts to optimize such a structure resulted in the previously discussed intermediates.

Electronic structures: The π molecular orbitals of the parent pyridinium ion **1 f** are illustrated in Figure 5. The presence of the N atom lowers the D_{6h} symmetry of benzene to C_{2v} for the pyridinium ion. However, the degenerate HOMO (e_{1g}) and

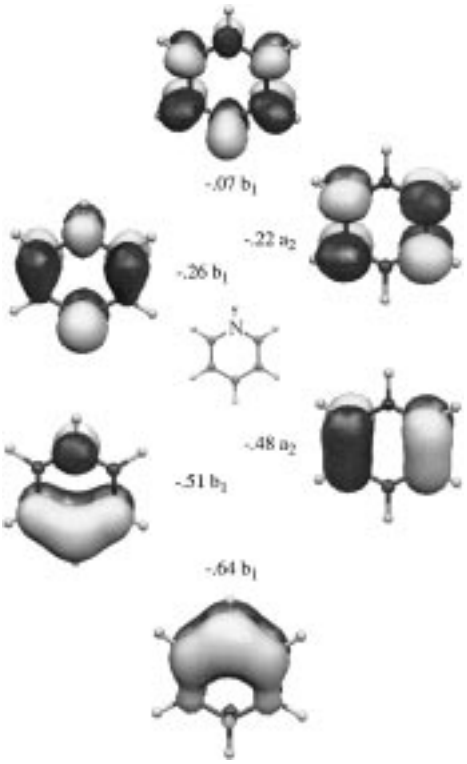

Figure 5. The π molecular orbitals of the pyridinium ion **1 f** computed at the 6-31G* B3LYP level of theory with their corresponding orbital eigenvalues. The N atom lies at the top of each orbital diagram.

LUMO (e_{2u}) of benzene are nearly degenerate for pyridinium. Two of the occupied π orbitals (those which have b_1 irreducible representations) are strongly shifted toward the N atom. Charge analyses reveal that the π electrons are shifted so much toward the N that the positive charge mainly resides on the C atoms. This highly polarized π density was noted by Del Bene and Jaffé[18] long ago.

Palmer et al.[20] have thoroughly examined the S_1 and S_2 photochemistry of benzene by means of MC-SCF methods, and fully characterized the Born–Oppenheimer violating regions. With regards to the electronic structure of "prefulvene", the benzene analogue of the *exo*-bicyclic ion **4 f**, the authors stated little other than describing its ground state as having a "quasidiradical nature", with one radical center on the allylic group and one on the out-of-plane C atom. However, in the case of the pyridinium ion, the increased nuclear charge of the N will strongly stabilize the closed-shell singlet configuration which possesses a lone pair on the N atom, relative to the diradical state. In fact, the use of unrestricted orbitals and varying orbital occupations in UHF or UB3LYP calculations does not substantially lower the energy of any of the structures studied from that with spin-restricted orbitals. For the *exo*-bicyclic ion **4 f**, proper treatment of the spin [two-configuration self-consistent field (TC-SCF) for an open-shell singlet and restricted open-shell Hartree–Fock, (ROHF) for a triplet] with the 3-21G basis set places the lowest open-shell singlet state and the lowest triplet state at 1.92 eV and 2.27 eV, respectively, above the spin-restricted energy of the closed-shell configuration. This result is in contrast with the claim of Sobolewski and Domcke based on STO-3G UHF calculations that the lowest energy state of prefulvene is the triplet state. For azoniabenzvalene **5 f**, the 3-21G UHF method (which is less theoretically justifiable but gives similar answers to those listed above for **4 f**) places the lowest open-shell singlet state and the lowest triplet state at 5.81 eV and 3.02 eV, respectively, above the closed-shell configuration.

Although the geometrical structure and relative energies of the pyridinium intermediates are somewhat similar to those of benzene, the electronic structure of the intermediates differs significantly. The closed-shell ground state of the *exo*-bicyclic ion **4 f** is seen to correlate adiabatically with the HOMO (a_2) → LUMO (b_1) doubly excited state of equilibrium pyridinium. This doubly excited state is initially unreachable upon excitation with light with $\lambda = 254$ nm (3-21G RHF places it 12.8 eV above equilibrium pyridinium). The dominant absorption in the experiments is the single $\pi \rightarrow \pi^*$ ($a_2 \rightarrow b_1$) excitation at 4.8 eV.[21] However, as the geometrical structure changes to that of the *exo*-bicyclic ion, the LUMO is strongly stabilized. The nodes of the LUMO on either side of the N atom (see Figure 5) are effectively eliminated by displacement of the N atom upward from the ring and toward the opposite C atom, and eventually occupation of this orbital becomes preferred. An electronic configuration which doubly occupies this orbital will be stabilized by the favorable interaction of the N lone pair of electrons being pointed toward the charged allylic group.

We have performed a cursory investigation of the S_1 surface with an open-shell-singlet SCF program and the 3-21G basis set. An optimized C_{2v} symmetry structure on S_1 has two imaginary frequencies for the b_1 irreducible representation and is a transition state along two reaction paths. Examination of the corresponding normal modes reveals that one of these reaction paths raises the N atom out of the plane of the six-membered ring, namely toward the *exo*-bicyclic ion **4 f**. (The other mode raises the opposite C atom out of the six-membered ring; however, nucleophilic attack on the resulting intermediate is not experimentally observed.) It remains an open question whether there is a barrier on S_1 (as for benzene) that must be overcome by excess vibrational energy to reach the state-crossing region of the PES and form the *exo*-bicyclic ion.

Reaction mechanism: Although we have not examined the Born–Oppenheimer violating regions in detail, the most important features of the photochemical mechanism are established by combining the structures and energies of the stationary points computed in this paper with the comprehensive theoretical treatments of benzene photoisomerization as well as the information known from experiment. All of these support a mechanism similar to that found in benzene;

$\pi \rightarrow \pi^*$ excitation results in rearrangement to *exo*-bicyclic ion **4** by a 2,6-bridging mechanism, followed by adiabatic motion on the ground-state PES. Depending on the precise nature of any substituents (see below), the bicyclic intermediate may pass over a barrier to azoniabenzvalene **5**. The azoniabenzvalene can then reopen into intermediate **4** in either of two ways, one of which results in the shift of the N atom by one position around the C ring.

A similar mechanism has recently been observed by Pavlik et al.[13] who reported the results of a series of experiments on the photochemistry of dimethylpyridines. The authors observed that product distributions from irradiation with $\lambda = 254$ nm (though not with $\lambda > 290$ nm) are consistent with a mechanism that involves electrocyclic ring closure, N migration, and rearomatization. Although Pavlik et al. claimed that there is no experimental evidence for the intermediacy of an azabenzvalene, the theoretical work on benzene and the pyridinium ion strongly suggests its presence.

The transition state between *exo*-bicyclic ion **4** and azoniabenzvalene **5** represents the bottleneck for N migration around the five-membered ring. Indeed, a low-lying transition state was found which connects the two intermediate structures and is shown in Figure 6. Beginning from **4a**, the

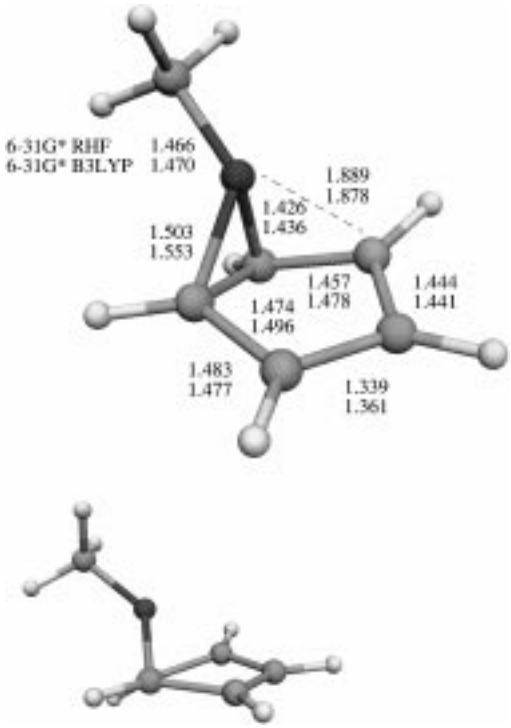

Figure 6. Geometrical structure (bond lengths in Å) of the C_1 symmetrical transition state between the *exo*-methyl bicyclic ion **4a** and the methylazoniabenzvalene **5a** intermediates.

transition state is characterized by a twisting of the C ring, a growing inequality in the length of the two previously allylic C–C bonds, and rotation of the methyl group. The result is that the distance of one of the allylic C atoms from the N atom is reduced from 2.3 to only 1.9 Å.

The relative energies of the computed stationary structures for the pyridinium **1f** and methylpyridinium ion **1a** are shown in Figures 7 and 8. The energies are corrected for zero-point vibrational energy and are given in kcal mol^{-1} relative to the ground state pyridinium at its equilibrium geometry. The energies given by RHF and B3LYP are consistent and predict that the *exo*-bicyclic ion **4f** lies below azoniabenzvalene **5f** by

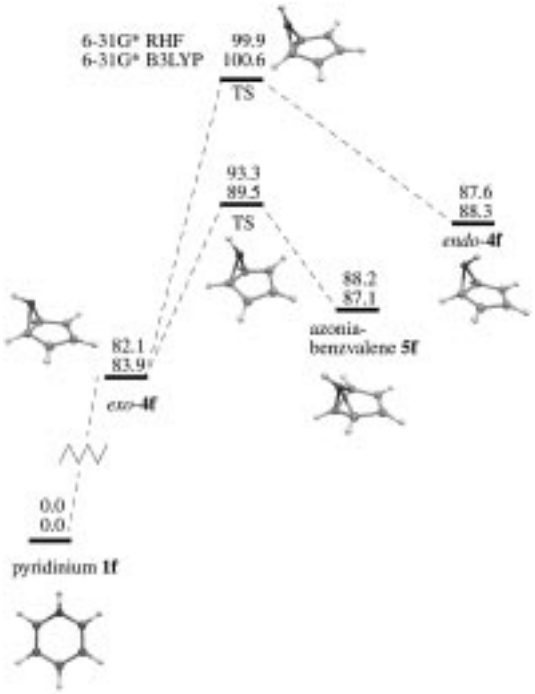

Figure 7. Relative energies [kcal mol^{-1}], corrected for zero-point vibrational energy, of stationary points on the pyridinium ground-state PES.

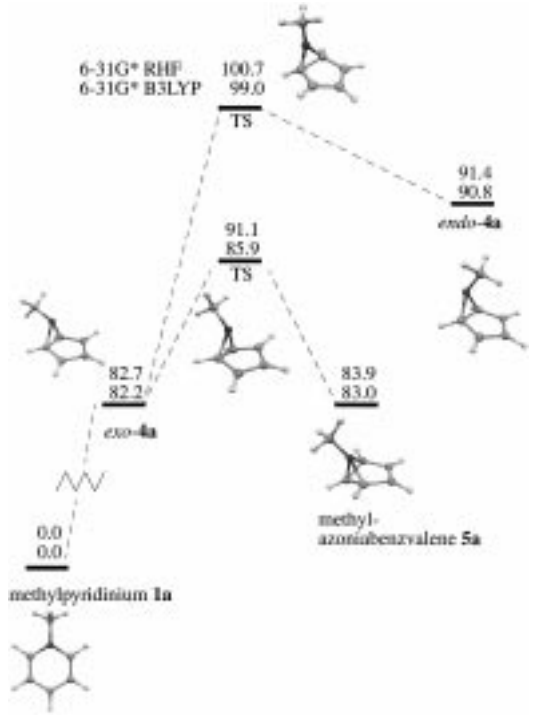

Figure 8. Relative energies [kcal mol^{-1}], corrected for zero-point vibrational energy, of stationary points on the methylpyridinium ground-state PES.

0947-6539/01/0708-1738 $ 17.50+.50/0 *Chem. Eur. J.* **2001**, *7*, No. 8

6.1 and 3.2 kcal mol^{-1}, respectively. This gap is reduced to $\approx$1 kcal mol^{-1} with both RHF and B3LYP for the corresponding methylpyridinium intermediates.

The largest difference between RHF and B3LYP occurs in the barrier height from the *exo*-bicyclic ion **4** to the azoniabenzvalene **5**, for which the RHF barrier is higher than the B3LYP barrier. These errors are rather typical for both of these methods, therefore, an average of the RHF and B3LYP barrier heights is a reasonable approximation to the actual barrier height. The barrier for the *exo*-bicyclic ion **4f** to form azoniabenzvalene **5f** is 11.2 kcal mol^{-1} and 5.6 kcal mol^{-1} with RHF and B3LYP, respectively. This barrier is reduced for the *N*-methylpyridinium intermediates to 8.4 kcal mol^{-1} with RHF and 3.7 kcal mol^{-1} with B3LYP.

The relative energies in Figures 7 and 8 are gas-phase values. We have computed the effect of solvation in water on the relative energies. The results are shown in Table 1. The isodensity surface-polarized continuum model (IPCM) of solvation that we have employed shows no significant change in the relative energies of the different pyridinium, intermediate, and transition-state structures. An increase of the critical barrier from the *exo*-bicyclic ion **4f** to the azoniabenzvalene **5f** of only 0.8 kcal mol^{-1} is predicted on account of solvation.

Table 1. Analysis of solvent effects on the relative energies of pyridinium conformations.[a]

Structure	Relative energy [kcal mol^{-1}] Gas phase		Aqueous	Difference
pyridinium **1f**	0.0	(0.0)	0.0	–
exo-bicyclic ion **4f**	86.8	(83.9)	85.8	−1.0
azoniabenzvalene **5f**	89.6	(87.1)	87.8	−1.8
exo-**4f** to **5f** transition state	92.7	(89.5)	92.5	−0.2
endo-bicyclic ion **4f**	91.2	(88.3)	87.6	−3.6
exo-**4f** to *endo*-**4f** transition state	104.7	(100.6)	105.7	+1.0

[a] Aqueous values were computed with 6-31G* B3LYP and the IPCM solvation model. The relative energies corrected for zero-point vibrational energy are given in parentheses (see also Figure 7).

We have also computed gas-phase thermochemical data for the hypothetical addition of hydroxide to the pyridinium ion **1f** to form the bicyclic aziridine **2f**. The results are shown in Table 2. Our most reliable computation of the free energy of the gas-phase reaction computed with large basis sets and B3LYP is −109.7 kcal mol^{-1}. Calculations with the 6-31++G* B3LYP level of theory and the IPCM solvent model results in solvation energies of −57.9 kcal mol^{-1} for pyridinium (which agrees precisely with experiment[22, 23]) and −8.9 kcal mol^{-1} for the aziridine product. The use of this solvation energy difference, along with the experimental solvation free energy of hydroxide of −106 kcal mol^{-1}[22, 23] results in an aqueous reaction free-energy of +45 kcal mol^{-1}.

Table 2. Gas-phase thermochemical data [kcal mol^{-1}] for the reaction pyridinium + hydroxide → 6-azabicyclo[3.1.0]hex-3-en-2-*exo*-ol.

	E[a]	H_{298}	G_{298}
3-21G RHF	−165.4	−163.2	−153.3
6-31G* RHF	−153.7	−151.0	−141.0
6-31++G* RHF	−127.8	−125.4	−115.4
6-311++G(3df,3pd) RHF//6-31++G*	−128.5	−126.1[b]	−116.1[b]
3-21G B3LYP	−182.5	−181.2	−171.4
6-31G* B3LYP	−159.8	−158.1	−148.2
6-31++G* B3LYP	−121.5	−120.2	−110.3
6-311++G(3df,3pd) B3LYP//6-31++G*	−120.9	−119.6[b]	−109.7[b]

[a] E is not corrected for zero-point vibrational energy. [b] Thermal correction taken from 6-31++G* computation.

The preference for *exo* products: As noted in the Introduction, **1a–e** form **2a–e** with both the N ligand and the OH group in *exo* orientations. As shown in Figures 7 and 8, if the N ligand is an H, then the *endo*-bicyclic ion is higher in energy than the *exo* form by $\approx$5 kcal mol^{-1}, while the presence of a bulky methyl group oriented toward the five-membered ring further destabilizes the *endo* form. However, whether the N ligand is H or CH_3, the transition state for *N*-pyramidalization between the *endo* and *exo* orientations lies 17 kcal mol^{-1} above the *exo* form. This value is in excellent agreement with barriers to nitrogen inversion reported for *N*-alkylaziridines.[24] The energy necessary is available only for a short time and is much larger than the barrier for N migration. We were unable to locate a second route to the *endo*-bicyclic ion via a transition state directly from the azoniabenzvalene intermediate.

Our calculations shed less light on the preference for *exo* orientation for the OH group in products **2**. As seen in Figure 2, as a result of the nearly orthogonal orientation of the two rings, the N atom represents significant steric hindrance to hydroxide attack on that face of the ring. Furthermore, the lone pair of electrons on the N will electrostatically repel an approaching anion. The opposite face of the five-membered ring is, however, perfectly accessible to nucleophilic attack.

Deuterium labeling experiments: For practical reasons, 3,4,5-trideuterio-*N*-(3-hydroxypropyl)pyridinium chloride ([D_3]**1b**) was chosen for the reinvestigation of labeling experiments (Scheme 2). The aziridine [D_3]**2b** that results from its photohydration at $\lambda = 254$ nm is considerably more stable and less prone to Grob fragmentation[2] than the *N*-methyl derivative used in the original work of Wilzbach et al.[1] Integration of the ^{1}H NMR spectrum of the isolated product [D_3]**2b** recorded at 500 MHz in CD_3OD provided the relative proton distribution over the five ring positions as given in Table 3. The assignment of the resonances was unambiguously established by a ^{13}C,^{13}C INADEQUATE-2D experiment[25] combined with the appropriate ^{1}H/^{13}C correlation. The interpretation of our results is based on the assumption that the photohydration reaction occurs without breaking any C–C bonds. Therefore, the three deuterium atoms of the starting material [D_3]**1b** remain neighbors in the product [D_3]**2b**, which is consequently a mixture of the isotopomers **9**, **10**, and **11**. The fact that less than 1% of the hydrogen in the starting material reaches position H–C3 of the product allows us to consider, in a first approximation, only a single 1,2-nitrogen shift, since its repetition would necessarily bring ^{1}H into position H–C3.

The dominant product **9** is clearly the result of 2,6-bridging of the starting pyridinium ion to the *exo*-bicyclic ion **6**

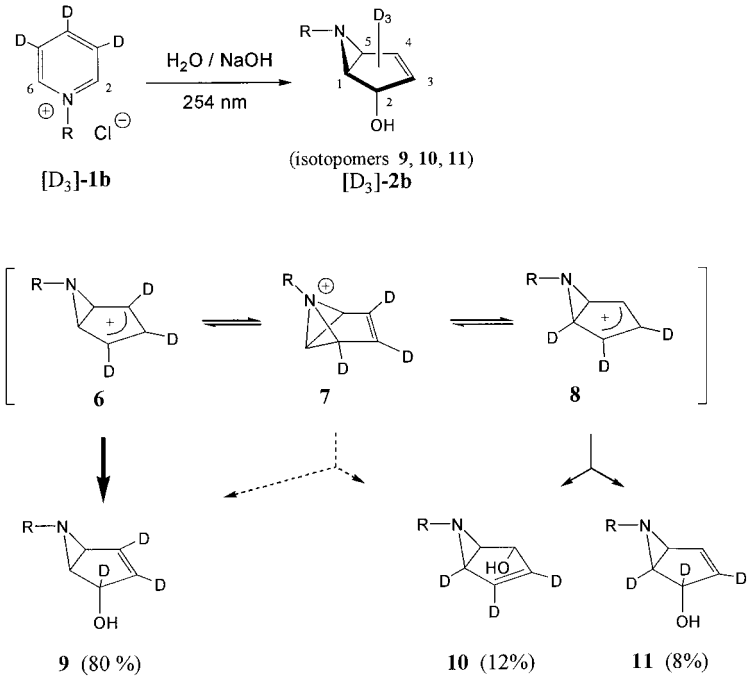

Scheme 2. Distribution of deuterium labeling for the photohydration of [D_3]**1b** and its interpretation [R = -$CH_2CH_2CH_2OH$].

Table 3. Distribution of ^{1}H over the five ring positions of [D_3]**2b** measured by ^{1}H NMR at 500 MHz in CD_3OD.

Position	^{1}H integral	δ^1H	δ^{13}C[a]	$T_1(^1H)$ [s][a]
H–C1	0.93	2.34	52.0	1.04
H–C2	0.12	4.17	75.5	2.65
H–C3	< 0.01	5.65	138.8	2.02
H–C4	0.08	6.03	135.3	2.62
H–C5	0.86	2.50	49.0	1.72

[a] Determined with unlabeled **2b**.

followed by immediate nucleophilic trapping. However, 20 % of the product, namely **10** and **11**, are evidence for N migration. We agree with the conjecture of Wilzbach et al.[1] that this migration occurs via the azoniabenzvalene **7**. Ion **7** may then reopen into either *exo*-bicyclic ion **6** or **8**. Nucleophilic attack on these allylic ions **6** and **8** roughly explains the observed product distribution. However, if it is assumed that ion **8** is the only origin of **10** and **11**, and isotope effects were negligible, then the product distribution of **10** and **11** should be equal. An interesting experimental observation is that they are not. In fact, the inequality may be explained by a fraction of the azoniabenzvalene **7** being intercepted directly by nucleophilic attack at its allylic bridgehead positions to give **9** and **10**. In summary, the results leave no doubt that 2,6-bridging of [D_3]**1b** to give the bicyclic ion **6** is the primary photochemical event and starting point of any further evolution.

Effect of *C*-methylation: As noted in the Introduction, experiments with *C*-methylated pyridinium salts indicate that methyl groups can exert a strong influence on the product distribution. Scheme 3 summarizes the products and relative yields reported for the photohydration of the picoline-derived pyridinium salts **12**, **16**, and **17**. For the reaction of 1,4-dimethylpyridinium chloride (**12**), the presence of the 4-methyl substituent is observed to have virtually no effect (relative to the unsubstituted *N*-methylpyridinium ion) on the product distribution. The main product **13** reflects 2,6-bridging, whereas the minor products **14** and **15** unveil a nitrogen shift. The photohydration of 1,3-dimethylpyridinium chloride (**16**) proceeds exclusively through 2,6-bridging to give **14** and **15**, again in a 1:1 ratio. Finally, the photohydrates of 1,2-dimethylpyridinium chloride (**17**), which are once again compounds **14** and **15**, result entirely from N migration.

This directive influence of the methyl substituents can be understood from the relative energies of the intermediates and transition states for unimolecular pyridinium rearrangement. Figure 9 contains a schematic PES for selected *N*-methylpyridinium ions with an additional *C*-methyl substituent. Although the RHF and B3LYP methods differ in their quantitative predictions of the energy barrier, they predict the same effects from methyl substitution. Starting from the 1,4-dimethylpyridinium ion (**12**), photoexcitation results in the *exo*-bicyclic structure with the methyl directly opposite to the N (right-hand side of Figure 9). Both RHF and B3LYP predict that the transition-state barrier to form the corresponding dimethyl-azoniabenzvalene is within 0.4 kcal mol^{-1} of the barrier in the unsubstituted *N*-methylpyridinium ion (compare with Figure 8). In fact, the resulting experimental product distribution is very similar, with 80 % of the product **13** resulting from 2,6-bridging and immediate nucleophilic attack. A minor difference is that **14** and **15** are produced in equal quantities. One possible explanation for this is to

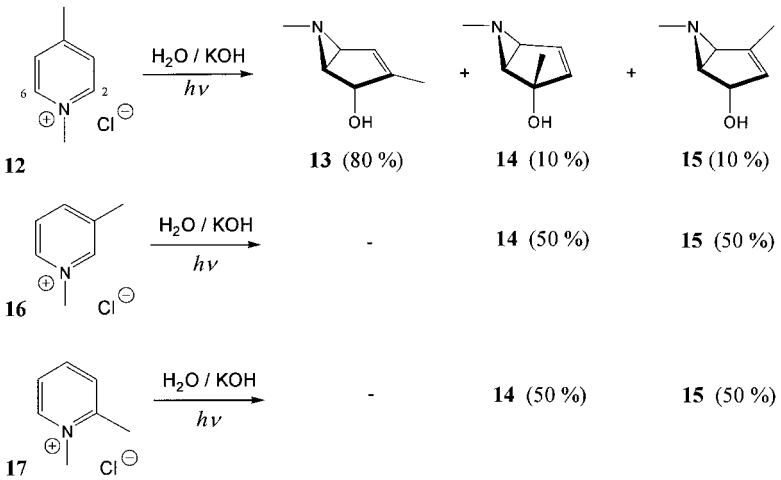

Scheme 3. Products and their relative yields reported for the photohydration of the picoline derivatives **12**[1, 26] (preparative yield 48 %), **16**,[1] and **17**.[1] Absolute yields for the reactions of **16** and **17** are not reported.

0947-6539/01/0708-1740 $ 17.50+.50/0 *Chem. Eur. J.* **2001**, *7*, No. 8

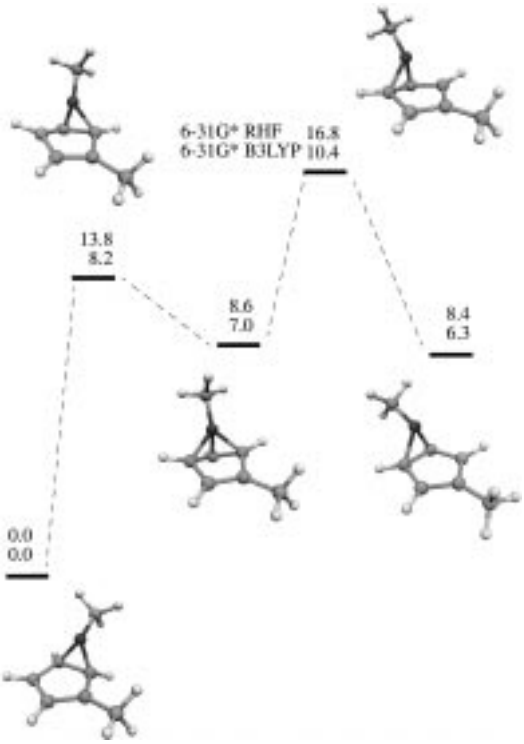

Figure 9. Schematic PES for methyl-substituted pyridinium intermediates.

assume equal probability of attack on the two allylic target atoms, but none at all on the benzvalene intermediate. This explanation is consistent with the computed energy barrier for the azoniabenzvalene to reopen toward the left in Figure 9; this barrier is reduced by the substituent methyl group from 2.9 to 1.2 kcal mol^{-1} at the 6-31G* B3LYP level of theory. Thus, in this case, the azoniabenzvalene may not survive for a sufficient length of time for it to be attacked.

Conversely, starting from the 1,3-dimethylpyridinium ion (**16**) (left-hand side of Figure 9) produces a different *exo*-bicyclic structure in which the methyl group strongly stabilizes the allylic cation. As a result, the barrier to formation of the azoniabenzvalene has been increased from 3.7 to 8.2 kcal mol^{-1} at the 6-31G* B3LYP level. Our computations clearly show that the great stability of the latter bicyclic allylic cation provides the key to the understanding of all of the N shifts observed in Scheme 3. We note (without computational support) that any intermediate bearing two vicinal methyl groups on an aziridine ring must be higher in energy, simply for reasons of steric congestion, than the lowest *exo*-bicyclic ion of Figure 9. This accounts for the reaction of the 1,2-dimethylpyridinium ion (**17**), and it does not come as a surprise, therefore, that the salts **16** and **17** lead to identical products.

In summary, the photolysis of *meta*-alkylated pyridinium salts occurs without N migration, whereas *para* substitution slightly favors, and *ortho* substitution very strongly favors the N shift. These directive influences hold not only for the picoline derivatives of Scheme 3 but also for the lutidinium salts of Scheme 4. Photohydration of 1,3,5-trimethylpyridinium chloride (**18**) gives exclusively the aziridine **19**.[1, 2] The same compound is obtained as the dominant product starting from 1,2,4-trimethylpyridinium chloride (**20**).[1]

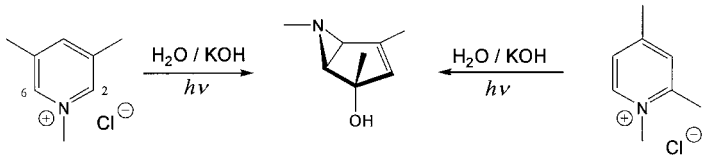

18 **19** **20**

Scheme 4. Products reported for the photohydration of the lutidine derivatives **18**[1] (preparative yield 71 %[2]) and **20**.[1] Absolute yield for the reactions of **20** is not reported.

Computational Methods

Various types of Hartree–Fock self-consistent field computations were performed including spin-restricted (RHF), unrestricted (UHF), restricted open-shell (ROHF), and two-configuration (TC-SCF) methods.[27] Various basis sets were used, including the 3-21G, the 6-31G*, and 6-311++G(3df,3pd) basis sets.[28, 29] Hartree–Fock stationary points were optimized by means of analytic first derivatives and characterized by analytic second derivatives.[30, 31] Density functional computations were performed with the B3LYP method comprised of the exchange functional of Becke[32] and the correlation functional of Lee, Yang, and Parr.[33] No spin-restriction was imposed on any of the reported B3LYP computations. The computations were performed with the PSI[34] and Gaussian[35] program packages. The figures were rendered with the MOLEKEL program.[36] The effect of the solvent on the computed relative energies has been calculated with the isodensity surface-polarized continuum model (IPCM).[37, 38] The gas-phase geometries were used for the solvent calculations. Lee et al.[39] have recently shown that the IPCM model successfully reproduces the solvation free-energy difference between the pyridinium ion and neutral pyridine in water.

Experimental Section

General: Photolyses: Srinivasan–Griffin reactor (Rayonet-RPR-100) with 16 RPR lamps, 2537 Å; double-walled quartz vessels with external cooling circuit (H_2O or MeOH). UV spectra: Kontron-Uvikon-860. IR spectra: Polaris-Mattson FT-IR spectrometer. NMR Spectra: Bruker Avance DRX-400 (9.4 Tesla), or Bruker Avance DRX-500 (11.74 Tesla); chemical shifts in organic solvents relative to internal $SiMe_4$; in D_2O relative to external 4,4-dimethyl-4-silapentane sodium sulfonate (DSS); explicit ^{13}C assignment is based on heteronuclear shift correlation; apparent scalar coupling constants J; multiplicities for ^{13}C according to DEPT or attached-proton test (ATP). MS: (*m*/*z* (% rel. to base peak)): VG-7070-E (EI) or Finnigan-SSQ-7000 (ESI) spectrometers; ESI-MS in MeOH.

Photohydration of [D_3]1b: 2,3,4,5,6-Pentadeuterio-*N*-(3-hydroxypropyl)-pyridinium chloride ([D_5]**1b**, 0.88 g, 5 mmol) prepared from [D_5]pyridine and 3-chloropropanol, as previously described for the unlabeled compound,[2] was dissolved in 0.5 M aqueous NaOH (50 mL). The solution was stirred for 24 h at room temperature in the dark to allow for D/H exchange in positions H–C2/H–C6.[40] An aliquot (20 mL) of this solution was deoxygenated (Ar) and irradiated ($\lambda = 254$ nm) with external water cooling for 16 h and then evaporated. Flash chromatography (basic alumina, CH_2Cl_2/MeOH saturated with NH_3 (20:1)) yielded [D_3]**2b** (253 mg, 80 %) as a yellowish oil which was consistent in its spectroscopic properties with unlabeled **2b**.[2] For label distributions see Table 3 and Scheme 2.

Acknowledgements

This research was supported by the Swiss National Science Foundation through grants 20–59263.99 and 20–54065.98. HFS acknowledges the support of the U.S. National Science Foundation.

[1] L. Kaplan, J. W. Pavlik, K. E. Wilzbach, *J. Am. Chem. Soc.* **1972**, *94*, 3283.

[2] F. Glarner, S. R. Thornton, D. Schärer, G. Bernardinelli, U. Burger, *Helv. Chim. Acta* **1997**, *80*, 121.

[3] E. A. Acar, F. Glarner, U. Burger, *Helv. Chim. Acta*, **1998**, *81*, 1095.
[4] R. Ling, M. Yoshida, P. S. Mariano, *J. Org. Chem*. **1996**, *61*, 4439.
[5] R. Ling, P. S. Mariano, *J. Org. Chem*. **1998**, *63*, 6072.
[6] S. J. Cho, R. Ling, A. Kim, P. S.Mariano, *J. Org. Chem*. **2000**, *65*, 1574.
[7] F. Glarner, B. Acar, I. Etter, T. Damiano, E. A. Acar, G. Bernardinelli, U. Burger, *Tetrahedron* **2000**, *56*, 4311.
[8] Review: A. Berecibar, C. Grandjean, A. Siriwardena; *Chem. Rev.* **1999**, *99*, 779.
[9] Reviews: a) M. T. Crimmins; *Tetrahedron* **1998**, *54*, 9229; b) T. S. Mansour, R. Storer, *Current Pharm. Design* **1997**, *3*, 227.
[10] a) C. S. Penkett, I. D. Simpson, *Tetrahedron* **1999**, *55*, 6183; b) C. S. Penkett, I. D. Simpson, *Synlett* **1999**, 93.
[11] U. C. Yoon, S. L. Quillen, P. S. Mariano, R. Swanson, J. L. Stavinoha, E. Bay, *J. Am. Chem. Soc*. **1983**, *105*, 1204.
[12] K. E. Wilzbach, D. J. Rausch, *J. Am. Chem. Soc*. **1970**, *92*, 2178.
[13] J. W. Pavlik, N. Kebede, M. Thompson, A. C. Day, J. A. Barltrop, *J. Am. Chem. Soc.* **1999**, *121*, 5666.
[14] I. Yamazaki, T. Murao, T. Yamanaka, K. Yoshihara, *Faraday Discuss. Chem. Soc*. **1983**, *75*, 395.
[15] S. Naqaoka, U. Nagashima, *J. Phys. Chem*. **1990**, *94*, 4467.
[16] D. E. Johnstone, J. R. Sodeau, *J. Phys. Chem*. **1991**, *95*, 165.
[17] M. C. Anthony, W. L. Waltz, P. G. Mezey, *Can. J. Chem.* **1982**, *60*, 813.
[18] J. Del Bene, H. H. Jaffé, *J. Chem. Phys.* **1968**, *49*, 1221.
[19] A. L. Sobolewski, W. Domcke, *Chem. Phys. Lett.* **1991**, *180*, 381.
[20] I. J. Palmer, I. N. Ragazos, F. Bernardi, M. Olivucci, M. A. Robb, *J. Am. Chem. Soc.* **1993**, *115*, 673.
[21] R. D. Brown, M. L. Heffernam, *Aust. J. Chem.* **1959**, *12*, 554.
[22] R. G. Pearson, *J. Am. Chem. Soc.* **1986**, *108*, 6109.
[23] S. Trassati, *Pure Appl. Chem.* **1986**, *58*, 955.
[24] J. B. Lambert, *Top. Stereochem*. **1971**, *6*, 52.
[25] A. Bax, R. Freeman, T. A. Frenkiel, *J. Am. Chem. Soc.* **1981**, *103*, 2102.
[26] D. Schärer, Ph.D. Thesis No. 2618, University of Geneva (Switzerland), **1993**.
[27] A. Szabo, N. S. Ostlund, *Modern Quantum Chemistry* McGraw – Hill, New York, **1989**.
[28] P. C. Hariharan, J. A. Pople, *Theor. Chim. Acta* **1973**, *28*, 213.
[29] W. J. Hehre, R. Ditchfield, J. A. Pople, *J. Chem. Phys.* **1972**, *56*, 2257.
[30] J. A. Pople, R. Krishnan, H. B. Schlegel, J. S. Binkley, *Int. J. Quantum Chem. Symp.* **1979**, *13*, 225.
[31] P. Saxe, Y. Yamaguchi, H. F. Schaefer, *J. Chem. Phys.* **1982**, *77*, 5647.
[32] A. D. Becke, *J. Chem. Phys.* **1993**, *98*, 5648.
[33] C. Lee, W. Yang, R. G. Parr, *Phys. Rev. B.* **1988**, *37*, 785.
[34] *PSI 2.0.8*, PSITECH, Inc., Watkinsville, GA 30677 (USA), **1995**; this program is generally available without charge.
[35] *Gaussian 94, Revision C.3*, Gaussian, Inc., Pittsburgh, PA (USA), **1995**.
[36] S. Portmann, H. P. Lüthi, *Chimia* **2000**, *54*, 766; http://www.cscs.ch/molekel
[37] S. Miertus, E. Scrocco, J. Tomasi, *Chem. Phys.* **1981**, *55*, 117.
[38] J. B. Foresman, T. A. Keith, K. B. Wiberg, J. Snoonian, M. J. Frisch, *J. Phys. Chem.* **1996**, *100*, 16098.
[39] I. Lee, C. K. Kim, I. S. Han, H. W. Lee, W. K. Kim, Y. B. Kim, *J. Phys. Chem. B* **1999**, *103*, 7302.
[40] J. A. Zoltewicz, G. M. Kaufmann, C. L. Smith, *J. Am. Chem. Soc.* **1968**, *90*, 5939.

Received: September 20, 2000 [F2741]

  0947-6539/01/0708-1742 $ 17.50+.50/0